White Dwarf Seismology

Michael Stroh

Overview

- History of White Dwarf Variables
- Types
- G-Modes
- White Dwarf Formation Channels
- What can we learn from power spectra?
- Common Mixing Length Theories
- What can we learn from spectra?

White Dwarfs

- Originally believed to be good standard candles
- In 1968, A.U. Landolt observed HL Tau 76
  - 12 minute period
  - Luminosity changed ~0.1 magnitudes
- Due to the size of WD populations, they are the most common type of variables
- >30 discovered

Variable WD Characteristics

- DAV
  - ‘ZZ Ceti’
  - 28 discovered (as of 2004)
  - Outer hydrogen envelope
  - Lie on an ‘instability strip’
  - 11,300K < T < 12,500K
- DBV
  - 8 discovered (as of 2004)
  - Outer He I envelope
  - 22,000K < T < 28,000K

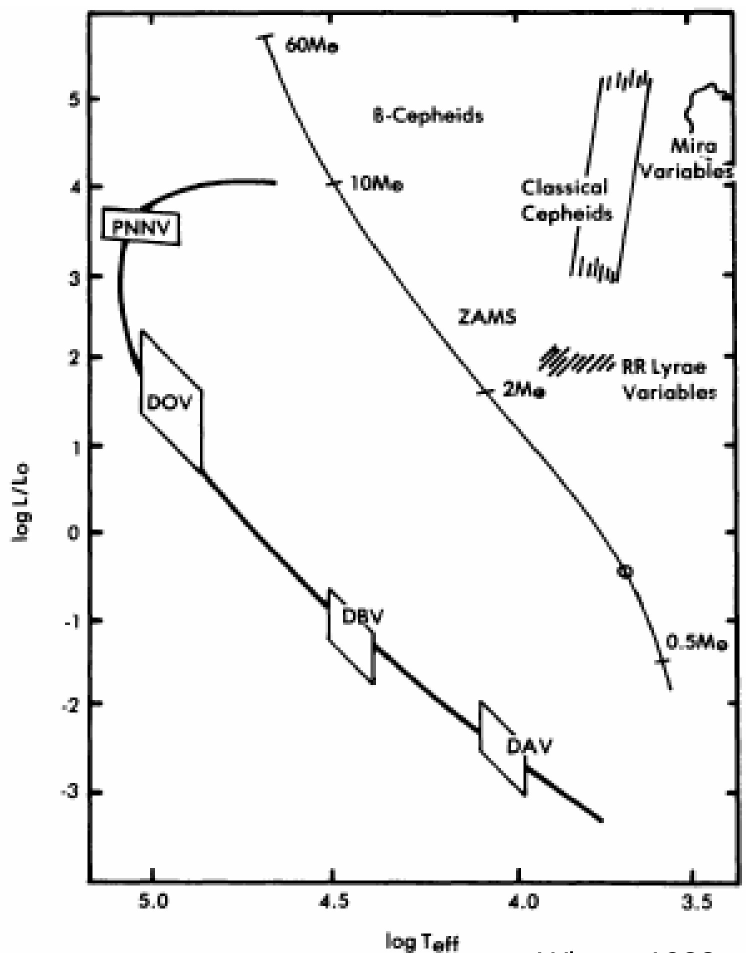

Winget 1988

Variable WD Characteristics

- DAV
  - ‘ZZ Ceti’
  - 28 discovered (as of 2004)
  - Outer hydrogen envelope
  - Lie on an ‘instability strip’
  - 11,300K < T < 12,500K
- DBV
  - 8 discovered (as of 2004)
  - Outer He I envelope
  - 22,000K < T < 28,000K

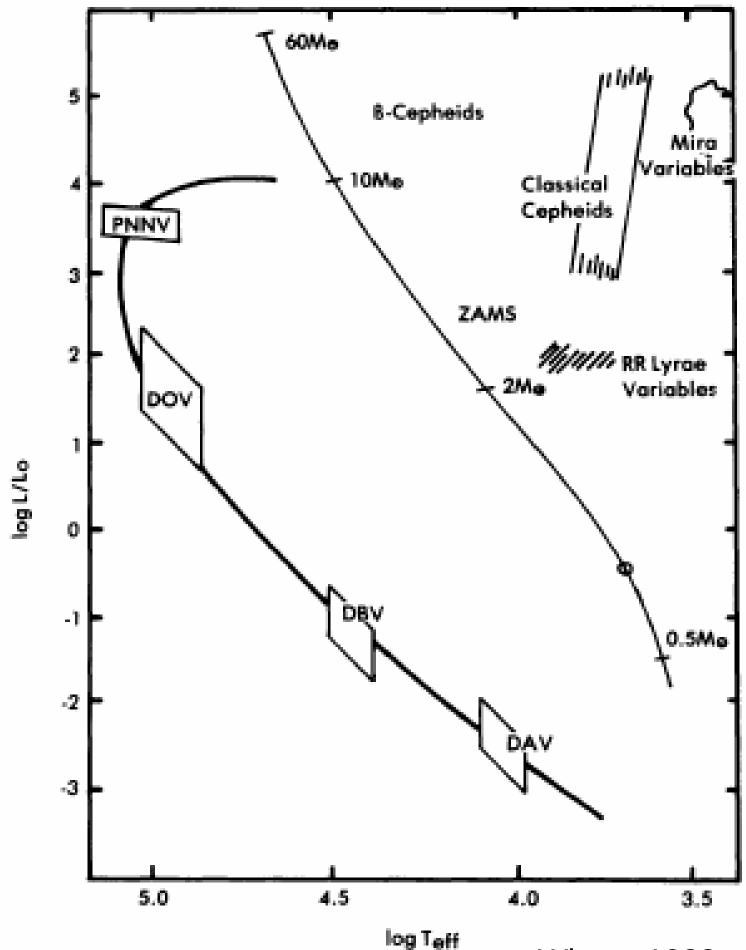

Winget 1988

- DOV / PNNV
  - Peculiar because spectroscopically similar objects not variable
  - 8×10^4 K < T < 1.7×10^5 K

Periods

Typical periods of WD variables are $10^2 – 10^3$s

For p-modes we have

$$\Pi_p \leq \pi \int \upsilon_s^{-1} ds$$

$$\approx \frac{0.04}{\sqrt{\frac{\langle \rho \rangle}{\langle \rho_{Sun} \rangle}}} days$$

For a typical white dwarf

$$\langle \rho \rangle \approx 10^6$$

$$\Pi_p \leq 4s$$

Therefore these cannot be the result of p-modes.

What else is there?

Gravity-modes

$$\Pi_g \approx n \frac{2\pi^2}{\sqrt{l(l+1)}} \left(\int_0^R \frac{N}{r} dr \right)^{-1}$$

Where the Brunt-Väisälä frequency, N, is given by

$$N^2 = -\frac{\chi_T}{\chi_\rho} (\nabla - \nabla_{ad}) \frac{g}{\lambda_p}$$

where

$$\chi_T \equiv \left(\frac{\partial \ln P}{\partial \ln T}\right)_\rho \quad \text{and} \quad \chi_\rho \equiv \left(\frac{\partial \ln P}{\partial \ln \rho}\right)_T$$

Numerical calculations produce observed periods.

G-Modes

$$\Pi_g \approx n \frac{2\pi^2}{\sqrt{l(l+1)}} \left(\int_0^R \frac{N}{r} dr \right)^{-1} = \frac{n\Pi_0}{\sqrt{l(l+1)}}$$

G-Modes

$$\Pi_g \approx n \frac{2\pi^2}{\sqrt{l(l+1)}} \left(\int_0^R \frac{N}{r} dr \right)^{-1} = \frac{n\Pi_0}{\sqrt{l(l+1)}}$$

$$N^2 = -\frac{\chi_T}{\chi_\rho} (\nabla - \nabla_{ad}) \frac{g}{\lambda_p}$$ Brunt-Väisälä frequency

G-Modes

$$\Pi_g \approx n \frac{2\pi^2}{\sqrt{l(l+1)}} \left(\int_0^R \frac{N}{r} dr \right)^{-1} = \frac{n\Pi_0}{\sqrt{l(l+1)}}$$

$$N^2 = -\frac{\chi_T}{\chi_\rho} (\nabla - \nabla_{ad}) \frac{g}{\lambda_p}$$

Brunt-Väisälä frequency

$$\chi_T \equiv \left(\frac{\partial \ln P}{\partial \ln T} \right)_\rho \rightarrow \frac{N_A k}{\mu_I} \frac{\rho T}{P_e}$$

G-Modes

$$\Pi_g \approx n \frac{2\pi^2}{\sqrt{l(l+1)}} \left(\int_0^R \tfrac{N}{r} dr \right)^{-1} = \frac{n\Pi_0}{\sqrt{l(l+1)}}$$

$$N^2 = -\frac{\chi_T}{\chi_\rho} (\nabla - \nabla_{ad}) \frac{g}{\lambda_p}$$ Brunt-Väisälä frequency

$$\chi_T \equiv \left(\frac{\partial \ln P}{\partial \ln T}\right)_\rho \rightarrow \frac{N_A k}{\mu_I} \frac{\rho T}{P_e}$$

$$\chi_\rho \equiv \left(\frac{\partial \ln P}{\partial \ln \rho}\right)_T \rightarrow \begin{cases} \frac{5}{3} & nonrelativistic \\ \frac{4}{3} & relativistic \end{cases}$$

G-Modes

$$\Pi_g \approx n \frac{2\pi^2}{\sqrt{l(l+1)}} \left(\int_0^R \frac{N}{r} dr \right)^{-1} = \frac{n\Pi_0}{\sqrt{l(l+1)}}$$

$$N^2 = -\frac{\chi_T}{\chi_\rho} (\nabla - \nabla_{ad}) \frac{g}{\lambda_p}$$ Brunt-Väisälä frequency

$$\chi_T \equiv \left(\frac{\partial \ln P}{\partial \ln T}\right)_\rho \rightarrow \frac{N_A k}{\mu_I} \frac{\rho T}{P_e}$$

$$\chi_\rho \equiv \left(\frac{\partial \ln P}{\partial \ln \rho}\right)_T \rightarrow \begin{cases} \frac{5}{3} & nonrelativistic \\ \frac{4}{3} & relativistic \end{cases}$$

Wave propagation theory suggests that in WDs

p-modes: deep interior

g-modes: envelope

What causes these instabilities?

- As with the classical variables, these are probably related to the ionization of hydrogen, helium and carbon.
- Winget et al. 1982b discovered the first DBVs which were previously predicted from theory.
- DAV and DBV star structure well understood
- DAVs typically only show a few g-modes.

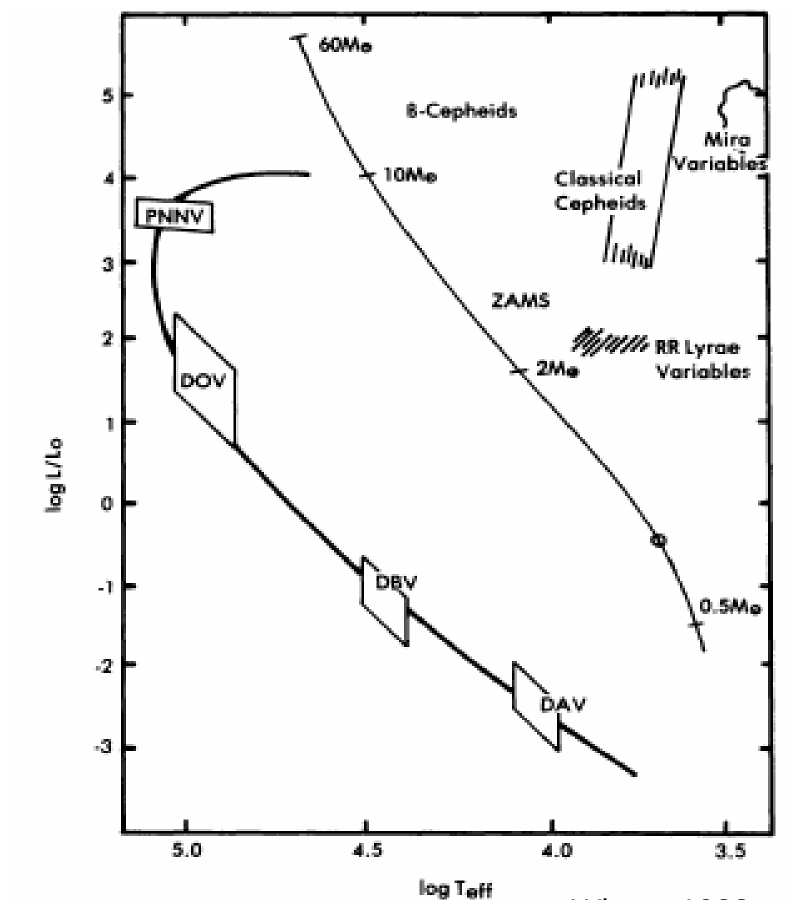

Winget 1988

DOV/PNNV Instabilities

- Not as well understood as DAVs and DBVs.
- Spectroscopic information not clear enough to determine compositions
- PNNs can be particularly difficult to observe due to their surroundings

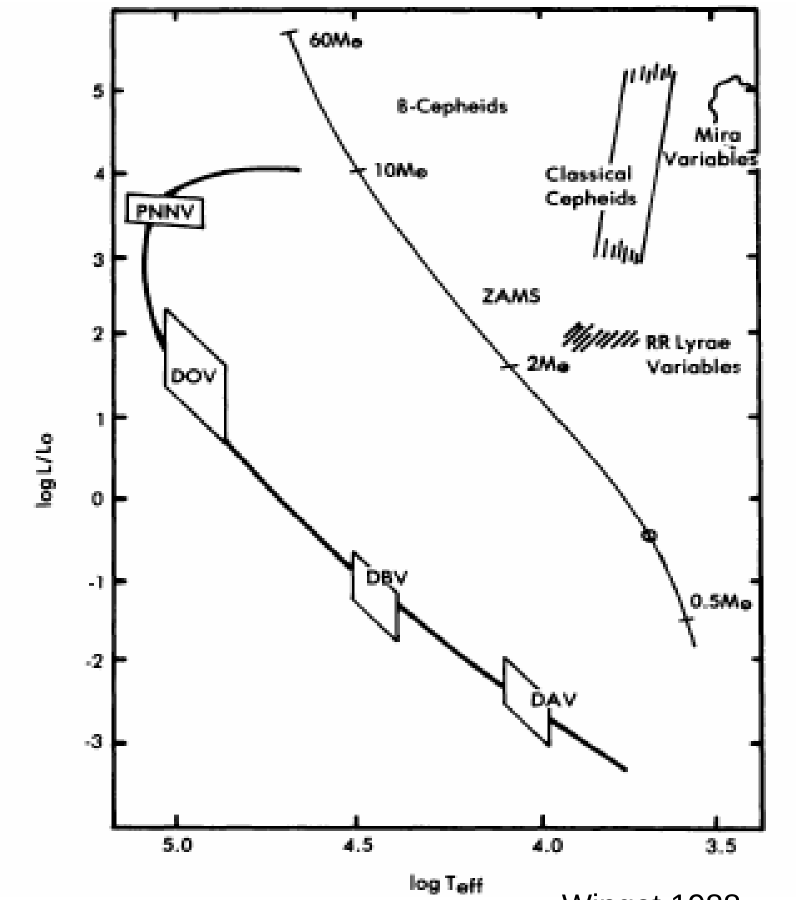

Winget 1988

White Dwarf Formation "Channels"

- "Born DA"
  - Result from hydrogen rich PNN
  - H shell ~$10^{-4}M_*$ *minus* what PNN wind stripped off
- He/C/O PNN that become DOVs
  - As star contracts and cools, H is diffused to the atmosphere
  - By 45,000K all stars have H shells
  - H shell ~$10^{-10}M_*$ - $10^{-4}M_*$
  - Recent evidence suggests this is not the major channel

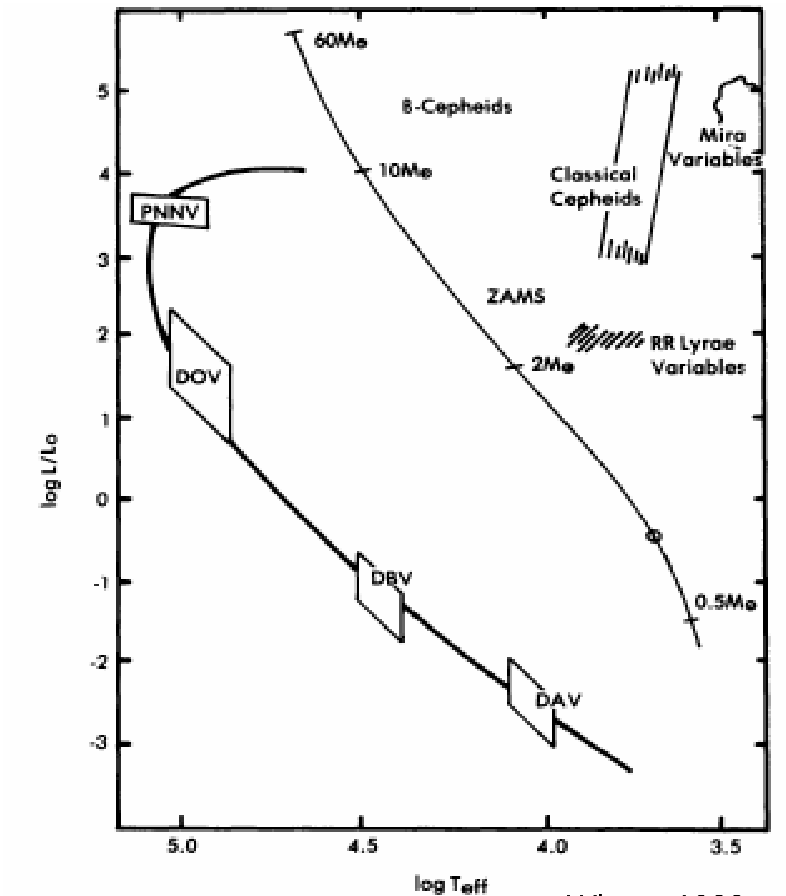

Winget 1988

10 Day Light Curve of PG 1159-035

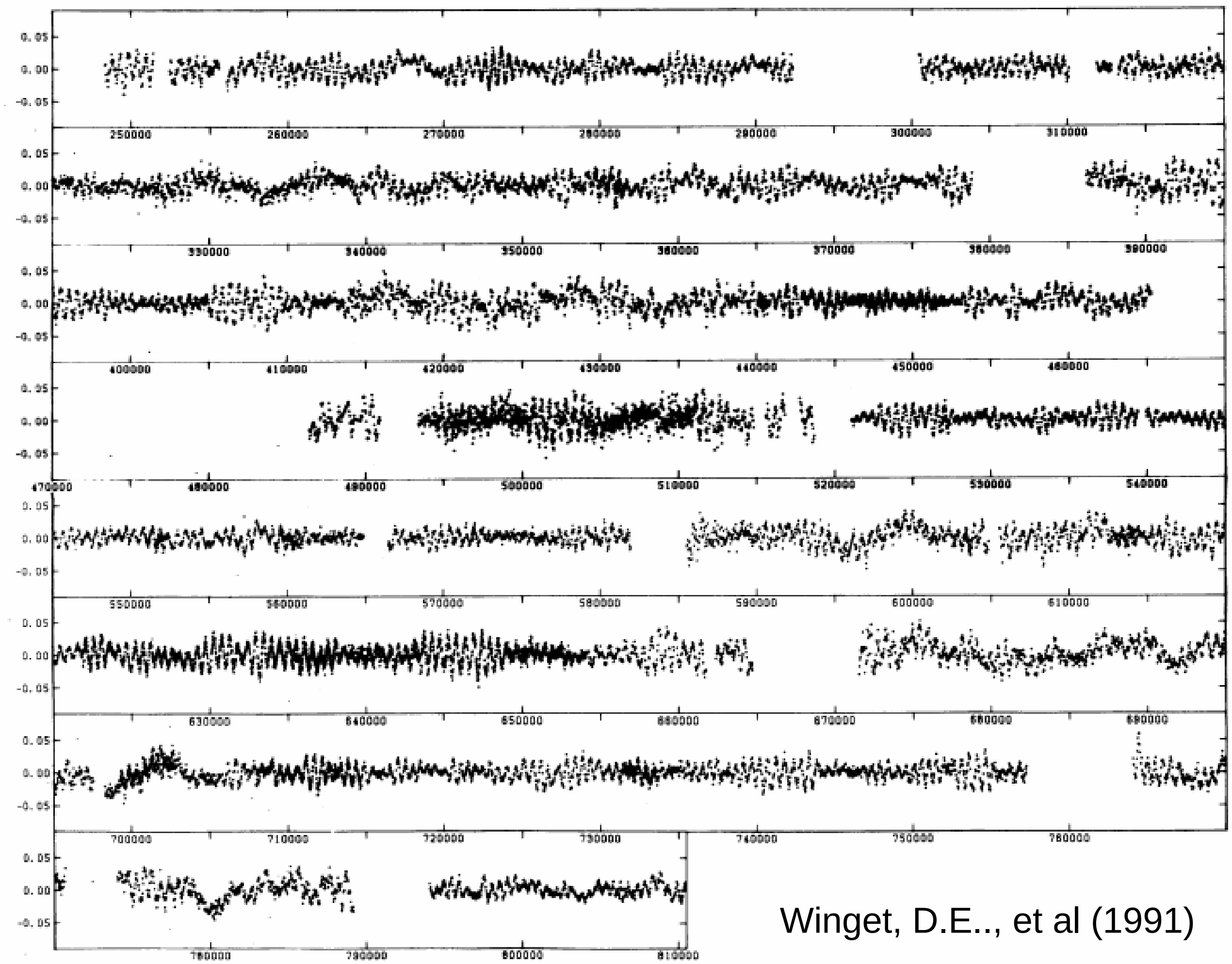

Winget, D.E.., et al (1991)

Power Spectrum of PG 1159-035

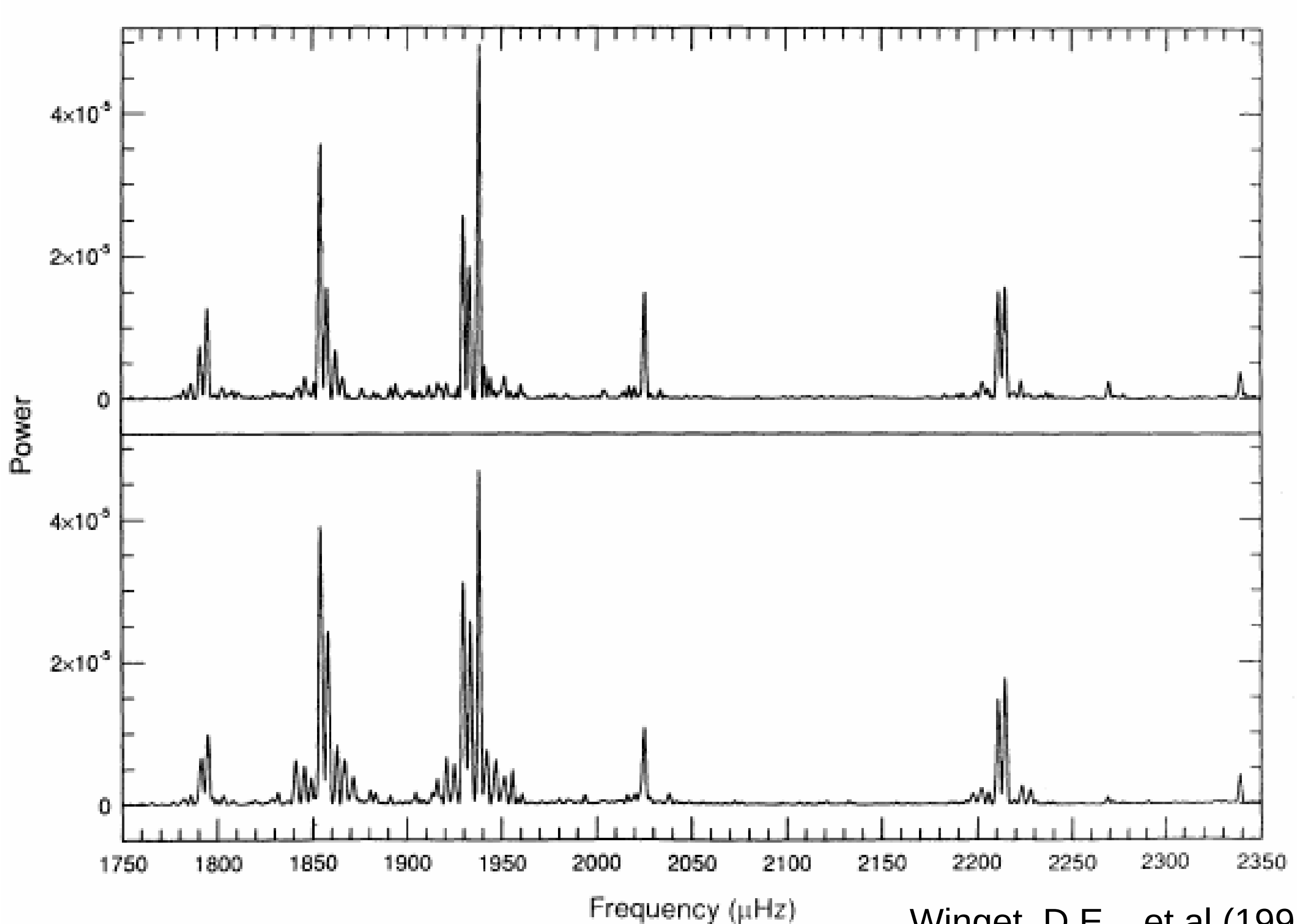

Winget, D.E.., et al (1991)

Power Spectrum of PG 1159-035

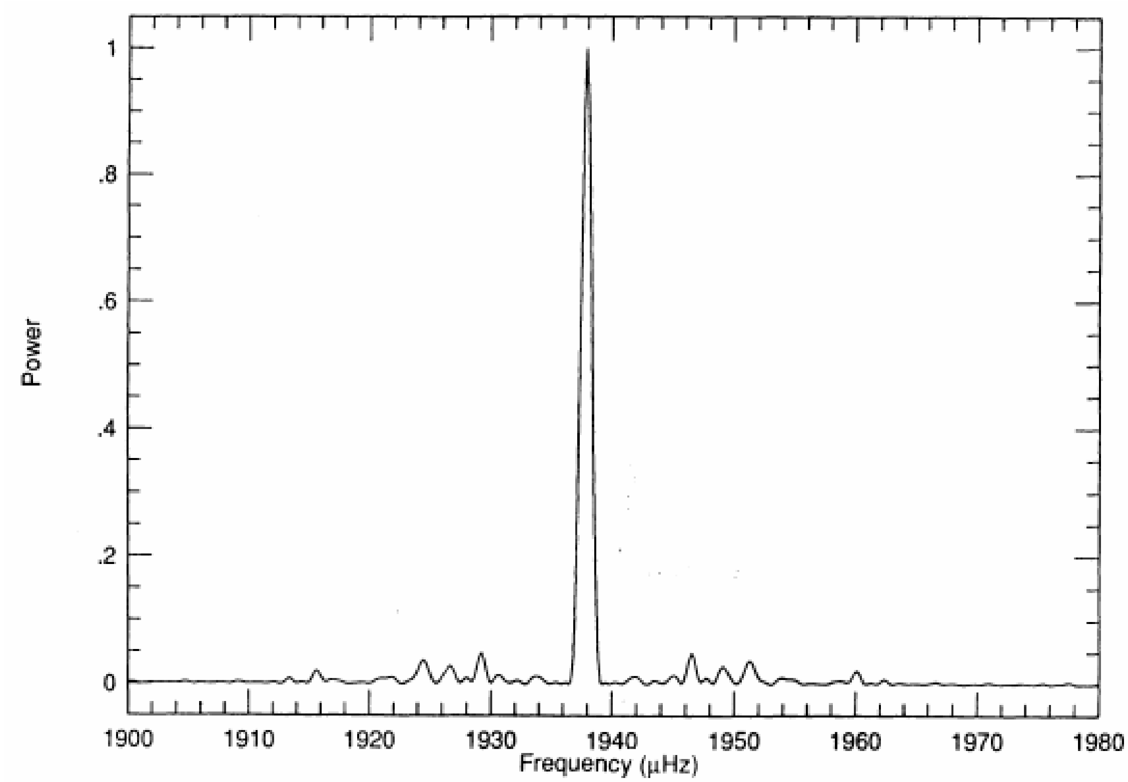

Winget, D.E.., et al (1991)

Power Spectrum of PG 1159-035

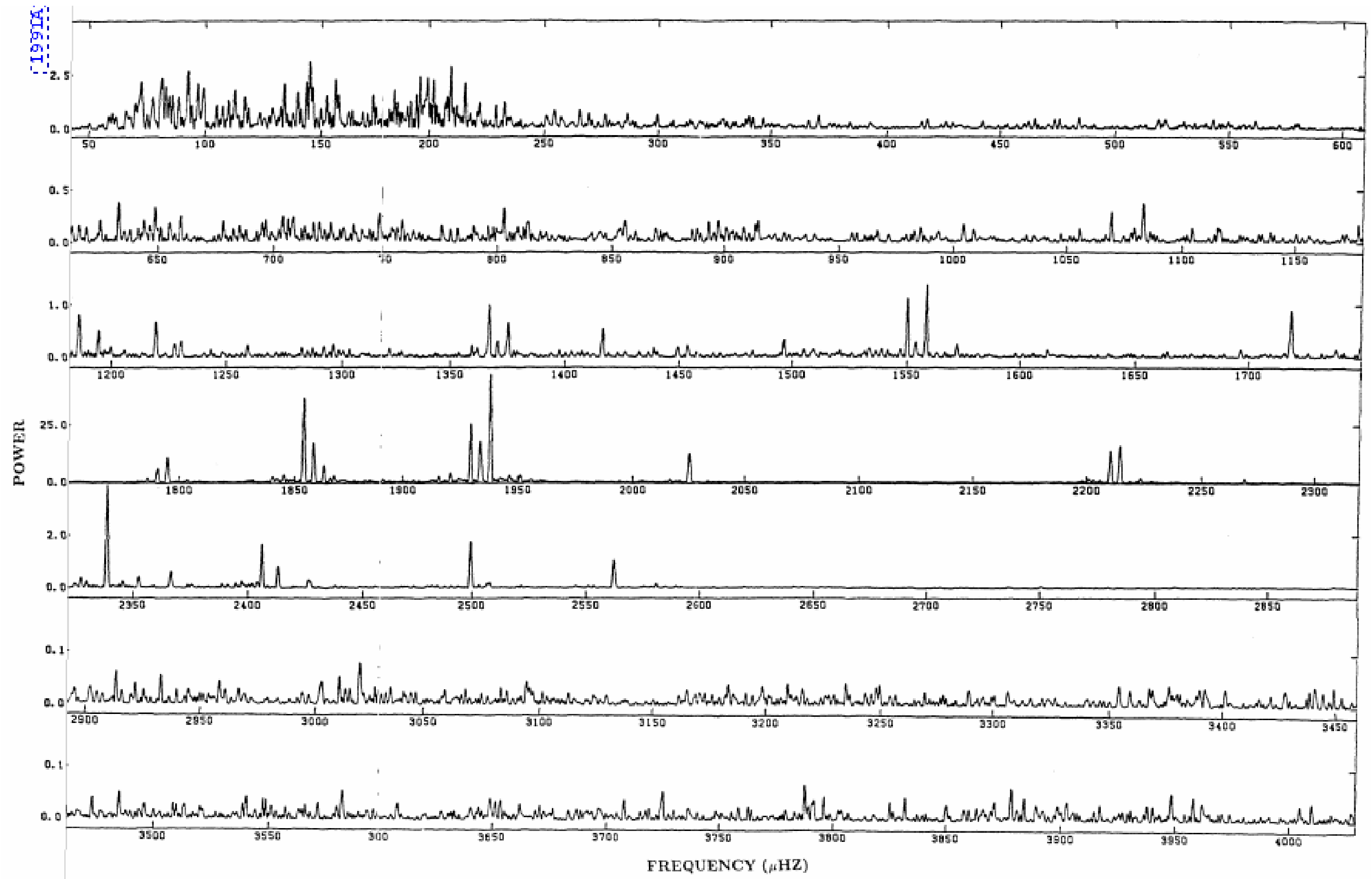

Winget, D.E.., et al (1991)

Power Spectrum of PG 1159-035

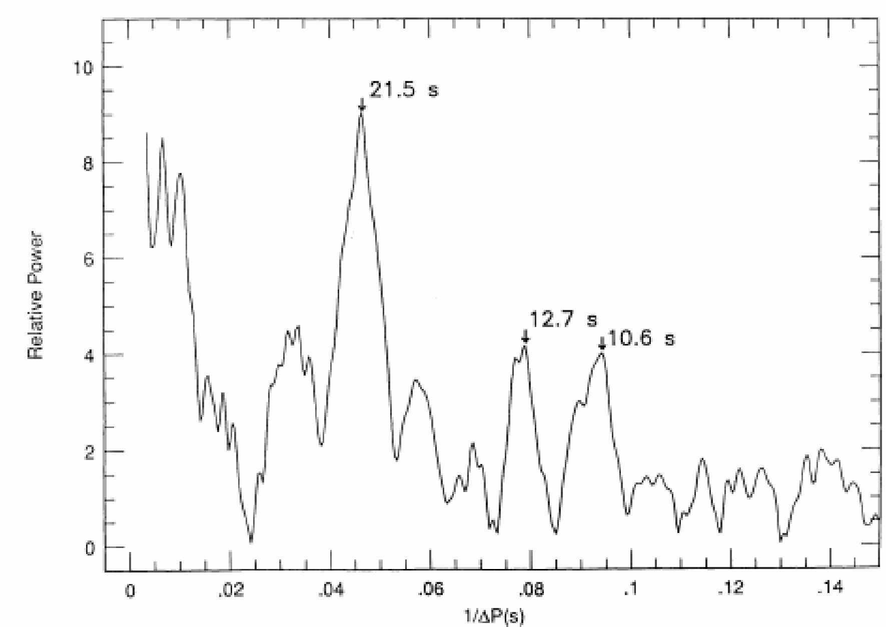

Winget, D.E.., et al (1991)

$$\Pi_g \approx \frac{n\Pi_0}{\sqrt{l(l+1)}}$$

Power Spectrum of PG 1159-035

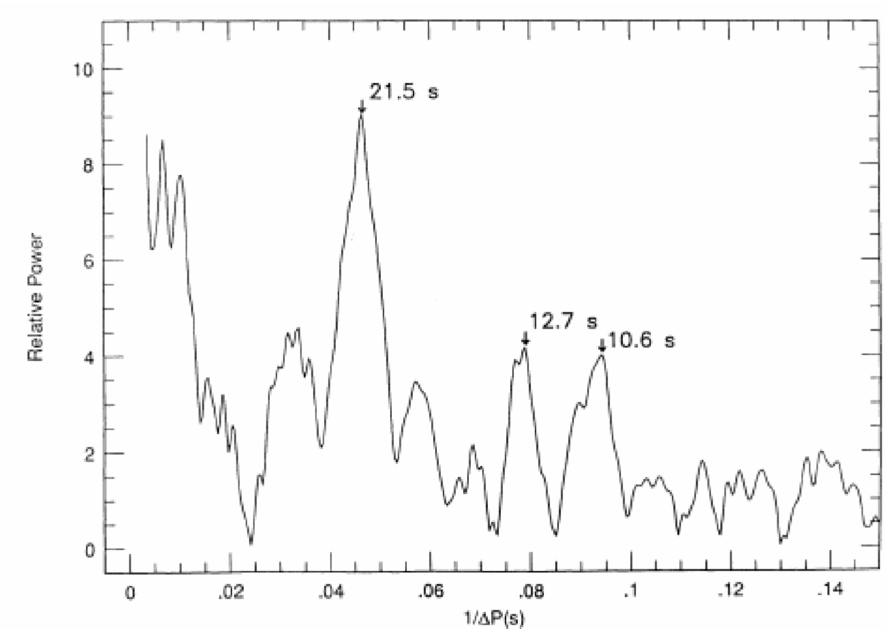

Winget, D.E.., et al (1991)

$$\Pi_g \approx \frac{n\Pi_0}{\sqrt{l(l+1)}}$$

Two observed periods

$$\frac{21.5s}{12.5s} = 1.72$$

Power Spectrum of PG 1159-035

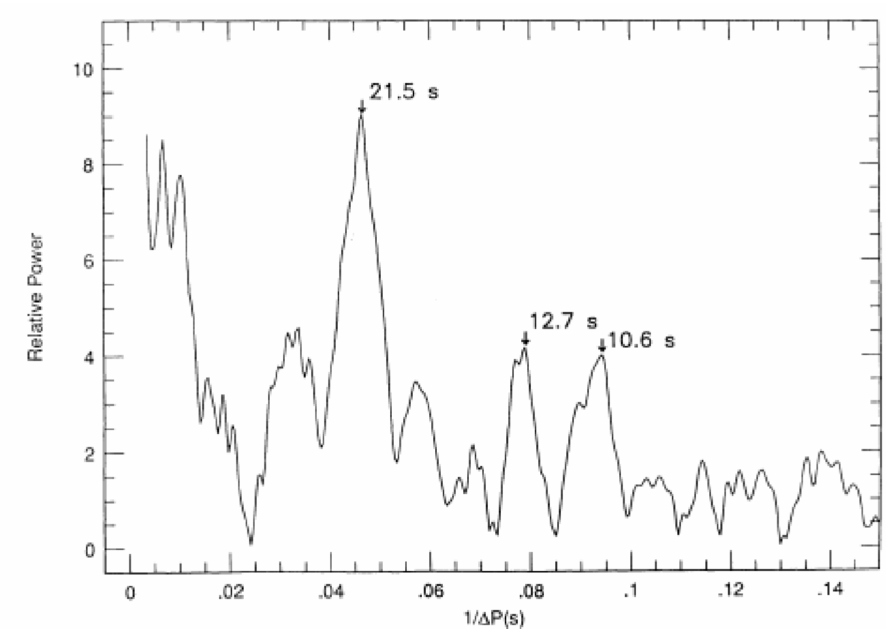

Winget, D.E.., et al (1991)

$$\Pi_g \approx \frac{n\Pi_0}{\sqrt{l(l+1)}}$$

Two observed periods $\frac{21.5s}{12.5s} = 1.72$

From theory $\frac{\Pi_{g,l=1}}{\Pi_{g,l=2}} = \frac{\sqrt{2(2+1)}}{\sqrt{1(1+1)}} = \sqrt{3} \approx 1.732$

Power Spectrum of PG 1159-035

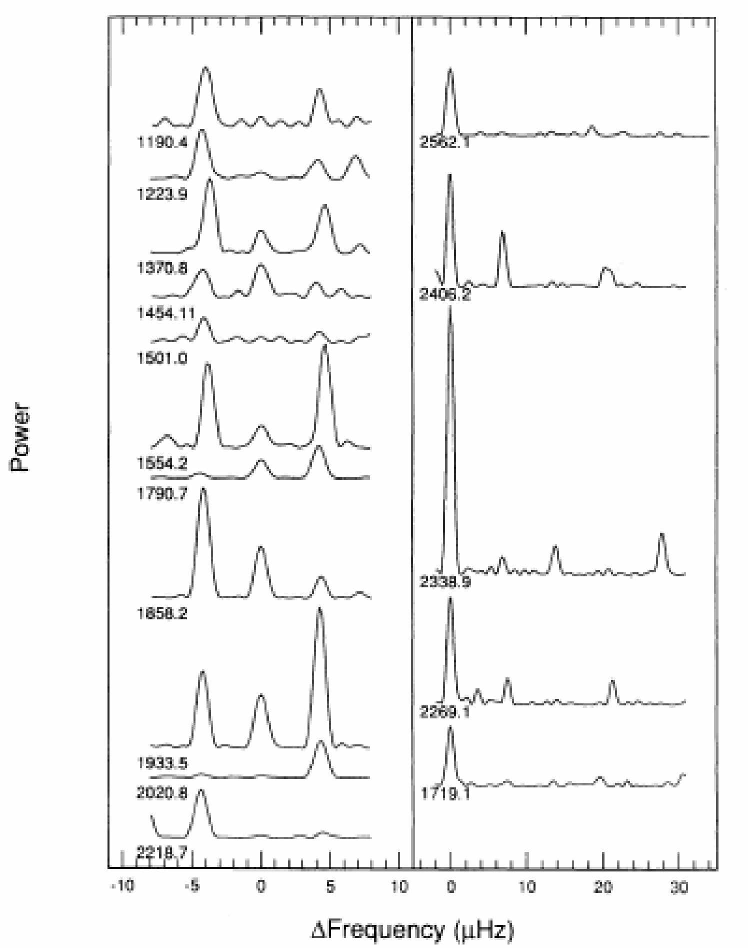

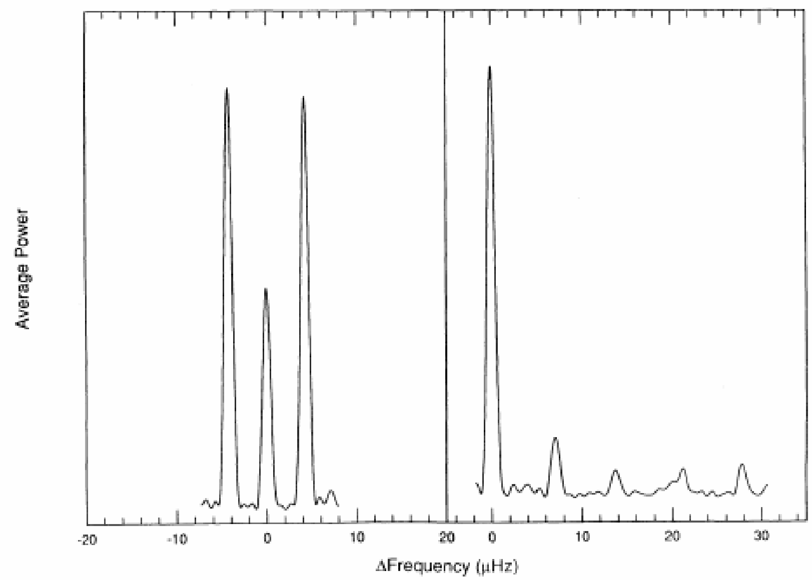

FIG. 6.—Average of the power in the multiplets shown in Fig. 4 for $l = 1$ (*left panel*) and $l = 2$ (*right panel*)

Winget, D.E.., et al (1991)

What causes the splitting?

Power Spectrum of PG 1159-035

- Rotation Period

$$P_{rot,l} = \frac{1 - \frac{1}{l(l+1)}}{\delta\upsilon_l}$$

Power Spectrum of PG 1159-035

- Rotation Period

$$P_{rot,l} = \frac{1 - \frac{1}{l(l+1)}}{\delta\upsilon_l}$$

$$\left.\begin{aligned} P_{rot,1} &= 1.371 \pm 0.13 days \\ P_{rot,2} &= 1.388 \pm 0.13 days \end{aligned}\right\} = 1.38 \pm 0.01 days$$

Power Spectrum of PG 1159-035

- Rotation Period

$$P_{rot,l} = \frac{1 - \frac{1}{l(l+1)}}{\delta\upsilon_l}$$

$$\left.\begin{aligned} P_{rot,1} &= 1.371 \pm 0.13 days \\ P_{rot,2} &= 1.388 \pm 0.13 days \end{aligned}\right\} = 1.38 \pm 0.01 days$$

- Mass

$$\log(\tfrac{M}{M_{Solar}}) = -1.041 \cdot \log\left\{\Pi_l \sqrt{l(l+1)}\right\} + 1.312$$

Power Spectrum of PG 1159-035

- Rotation Period

$$P_{rot,l} = \frac{1 - \frac{1}{l(l+1)}}{\delta\upsilon_l}$$

$$\left.\begin{aligned} P_{rot,1} &= 1.371 \pm 0.13 days \\ P_{rot,2} &= 1.388 \pm 0.13 days \end{aligned}\right\} = 1.38 \pm 0.01 days$$

- Mass

$$\log(\tfrac{M}{M_{Solar}}) = -1.041 \cdot \log\left\{\Pi_l \sqrt{l(l+1)}\right\} + 1.312$$

$$\tfrac{M}{M_{Solar}} = 0.586 \pm 0.003$$

Chemical Stratification of PG 1159-035

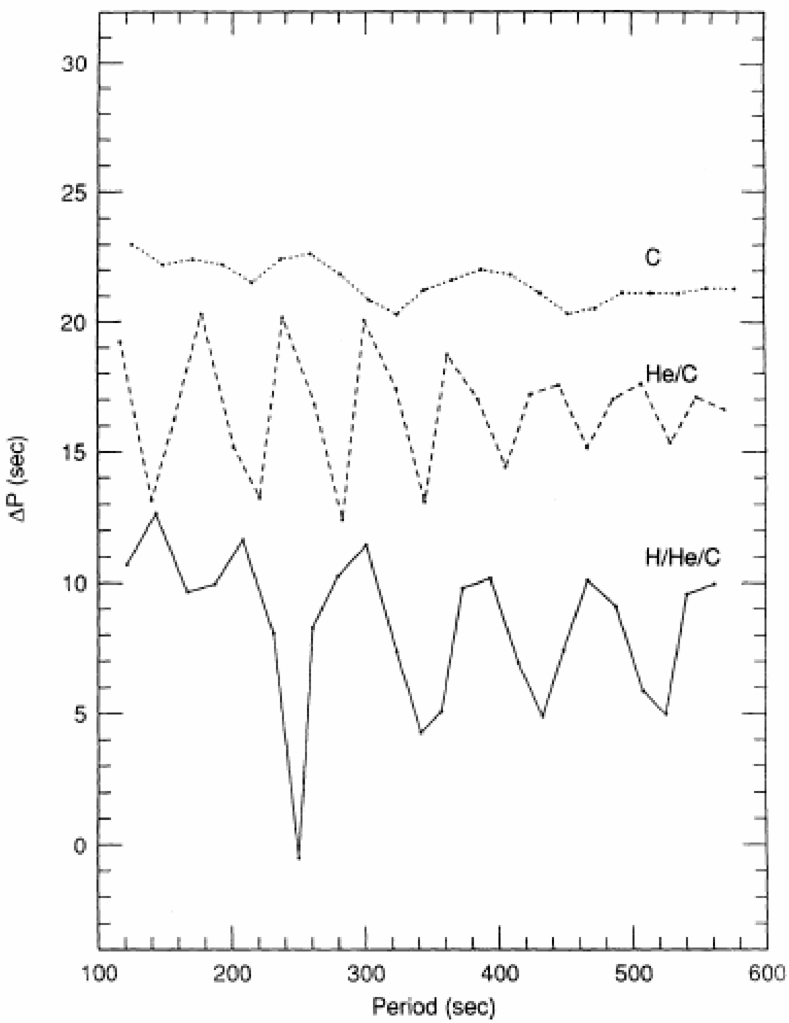

FIG. 9.—Theoretical period spacings (for $l = 1$ modes) for three different models, displaced vertically for clarity.

Winget, D.E.., et al (1991)

Chemical Stratification of PG 1159-035

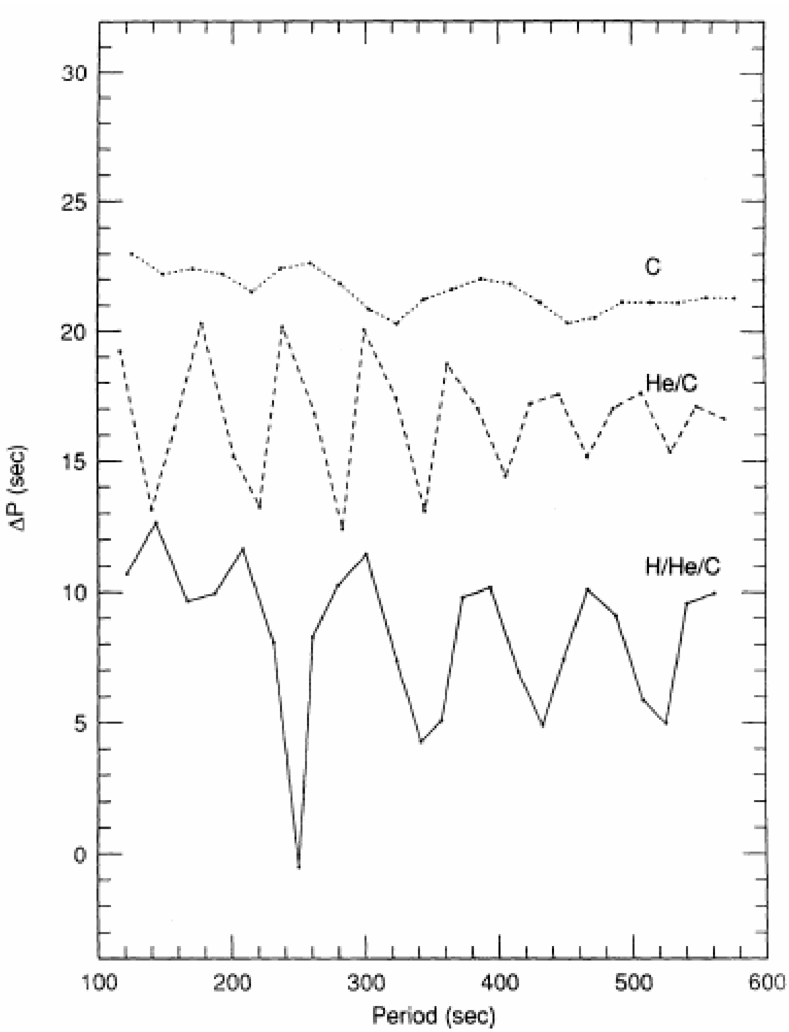

FIG. 9.—Theoretical period spacings (for $l = 1$ modes) for three different models, displaced vertically for clarity.

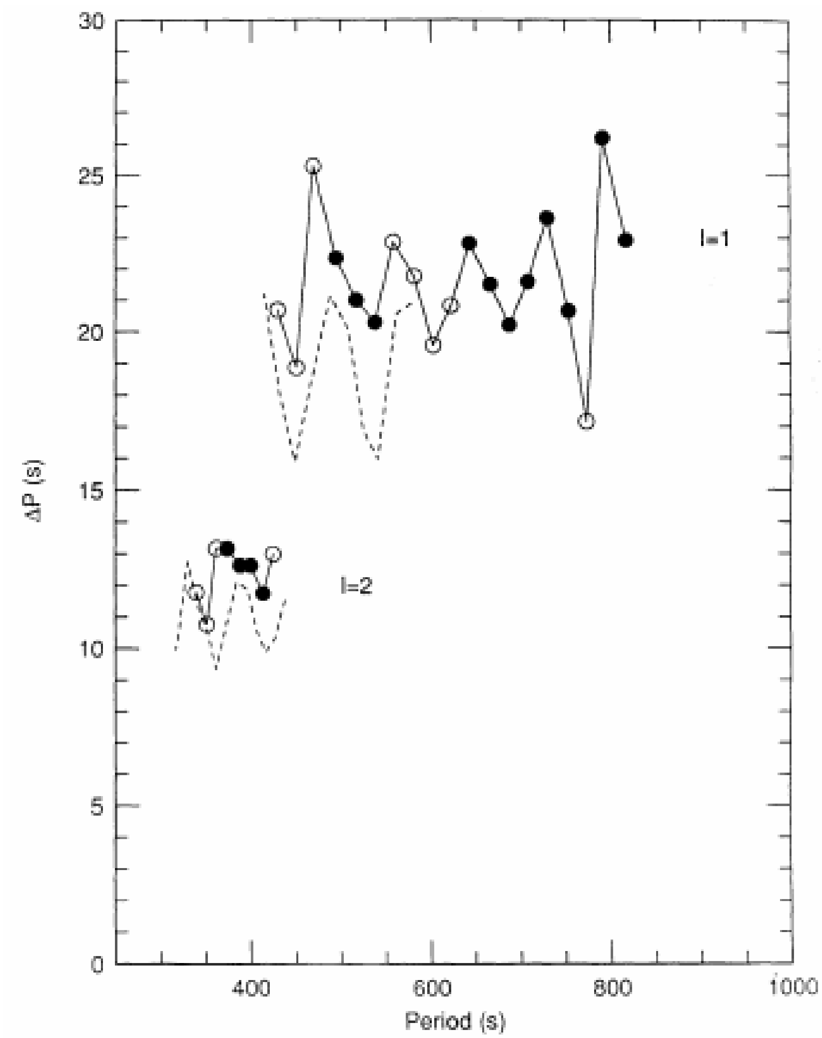

FIG. 10.—Observed period spacings in PG 1159−035. Open circle values are less certainly determined than those for the solid circles. The dashed lines show the theoretical trapping found in the H/He/C model. A small decrease in the model's mass would displace the dashed curves upward.

Winget, D.E.., et al (1991)

Period Variability

- Are these periods constant?

$$\frac{dP}{dt} = (-2.4 \pm 0.4) \cdot 10^{-11} s \cdot s^{-1}$$

$$(O - C) = T_{\max}^{obs} - T_0 - P \cdot E - \tfrac{P}{2} \dot{P} E^2$$

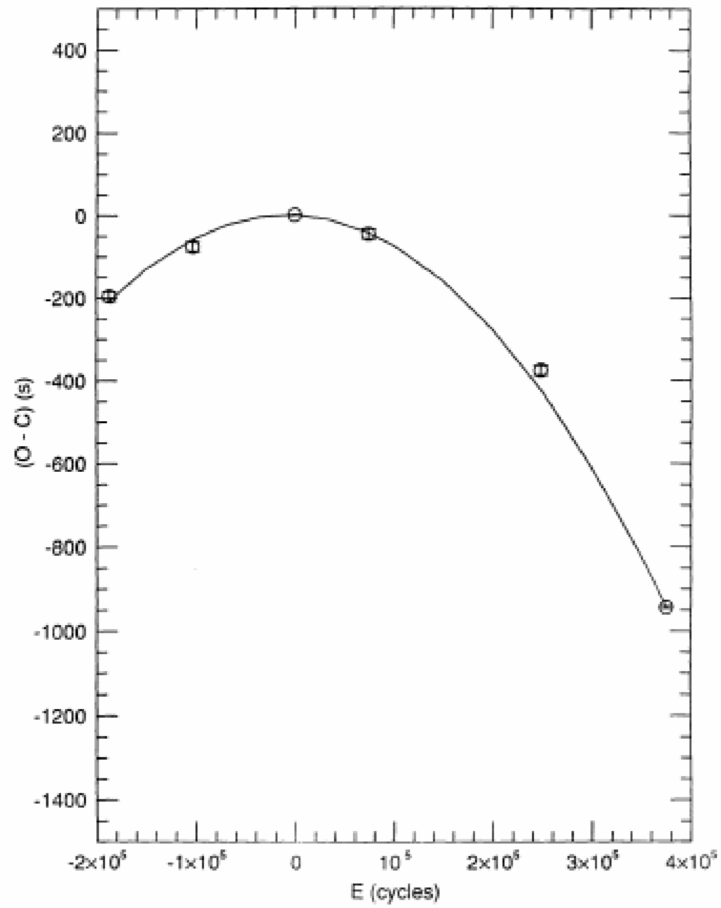

FIG. 11.—Observed phase of the 516 s period as a function of time (*circles*) with formal error bars shown. The solid curve is the phase ephemeris derived from the first four data points.

Winget, D.E.., et al (1991)

Period Variability

- Are these periods constant?

$$\frac{dP}{dt} = (-2.4 \pm 0.4) \cdot 10^{-11} s \cdot s^{-1}$$

$$(O - C) = T_{\max}^{obs} - T_0 - P \cdot E - \tfrac{P}{2} \dot{P} E^2$$

$$T_0 = (2445346.873562 \pm 0.000017) BJDD$$

$$P = 516.02531 \pm 0.00006 s$$

$$\frac{dP}{dt} = (-2.49 \pm 0.06) \cdot 10^{-11} s \cdot s^{-1}$$

BJDD (Barycentric Julian Dynamical Date)

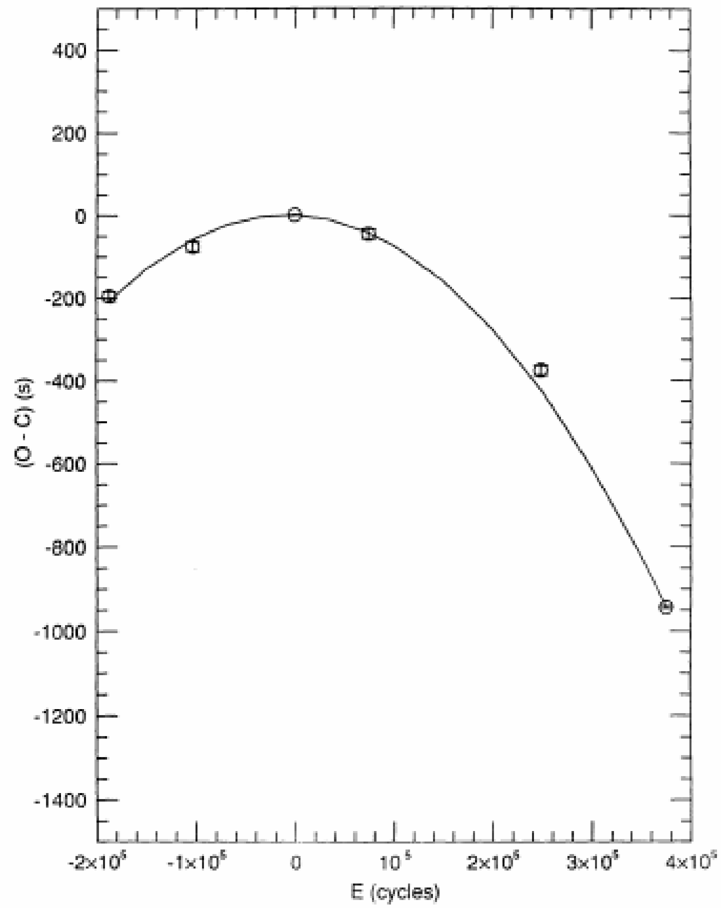

FIG. 11.—Observed phase of the 516 s period as a function of time (*circles*) with formal error bars shown. The solid curve is the phase ephemeris derived from the first four data points.

Winget, D.E.., et al (1991)

Mixing Length Theory

$$\alpha \equiv \frac{l}{H}$$

H is the pressure scale height and l is the mixing length

- ML1
  - α = 1
- ML2
  - α = 1
  - Increased convective efficiency relative to ML1
- ML3
  - Same as ML2 but α = 2
- ML2/$\alpha = 0.6$
  - Same as ML2 but α = 0.6

DAVs

- Using spectroscopy for a given filter x

$$a_1^x = A_l^x \varepsilon_T T_0 \overline{Y}_l^{\,m}(i)$$

a is the amplitude of a g-mode in the Fourier spectrum
ϵ is the dimensionless amplitude of the temperature perturbation
T_0 is the unperturbed effective temperature
Y_l^m is the Legendre function corresponding to an angle i

$$A_l^x \equiv \frac{\int_0^\infty W_\upsilon^x A_{l\upsilon} \frac{d\upsilon}{\upsilon}}{\int_0^\infty W_\upsilon^x H_{\upsilon,0} \frac{d\upsilon}{\upsilon}} \times 100 \qquad A_{l\upsilon} \equiv \frac{1}{2}\int_0^1 \left.\frac{\partial I_\upsilon}{\partial T}\right|_{T_0} P_l(\mu)\mu d\mu$$

W_ν^x is transmission function for filter x
$H_{0,\nu}$ is the unperturbed emergent Eddington flux
I_ν is the emergent specific intensity
$P_l(\mu)$ is the Legendre polynomial

DAVs

- Using spectroscopy for a given filter x

$$a_1^x = A_l^x \varepsilon_T T_0 \overline{Y}_l^{\,m}(i)$$

a is the amplitude of a g-mode in the Fourier spectrum
ϵ is the dimensionless amplitude of the temperature perturbation
T_0 is the unperturbed effective temperature
Y_l^m is the Legendre function corresponding to an angle i

$$A_l^x \equiv \frac{\int_0^\infty W_\upsilon^x A_{l\upsilon} \frac{d\upsilon}{\upsilon}}{\int_0^\infty W_\upsilon^x H_{\upsilon,0} \frac{d\upsilon}{\upsilon}} \times 100$$

$$A_{l\upsilon} \equiv \frac{1}{2} \int_0^1 \left. \frac{\partial I_\upsilon}{\partial T} \right|_{T_0} P_l(\mu) \mu d\mu$$

W_ν^x is transmission function for filter x
$H_{0,\nu}$ is the unperturbed emergent Eddington flux
I_ν is the emergent specific intensity
$P_l(\mu)$ is the Legendre polynomial

$$\frac{a_1^x}{a_1^y} = \frac{A_l^x}{A_l^y}$$

Behavior of A_l^x and the Pulsation Amplitude

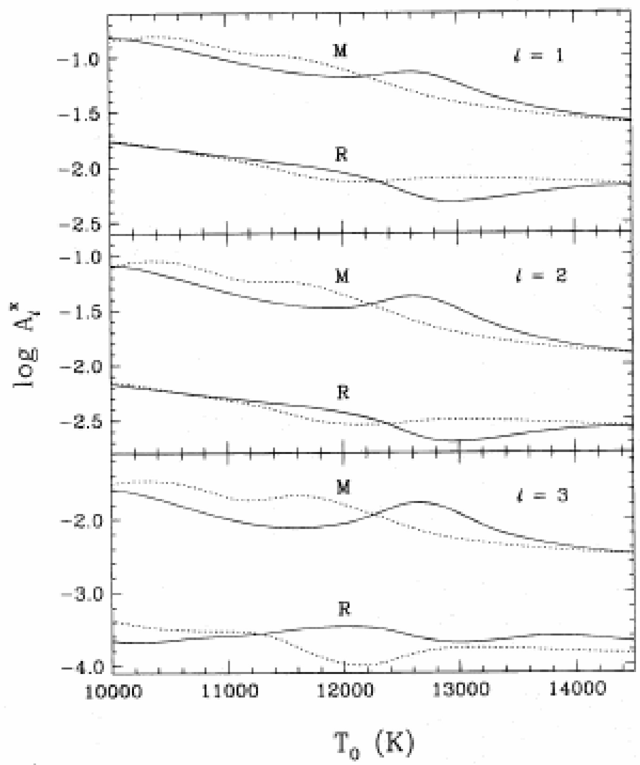

FIG. 1.—Behavior of the coefficient A_l^x for the M and R bandpasses in terms of unperturbed effective temperature at fixed surface gravity (log $g = 8.0$) for ML1 (*dashed curves*) and ML2 (*solid curves*) models. Each panel refers to a specific value of the pulsation index l, from 1 through 3.

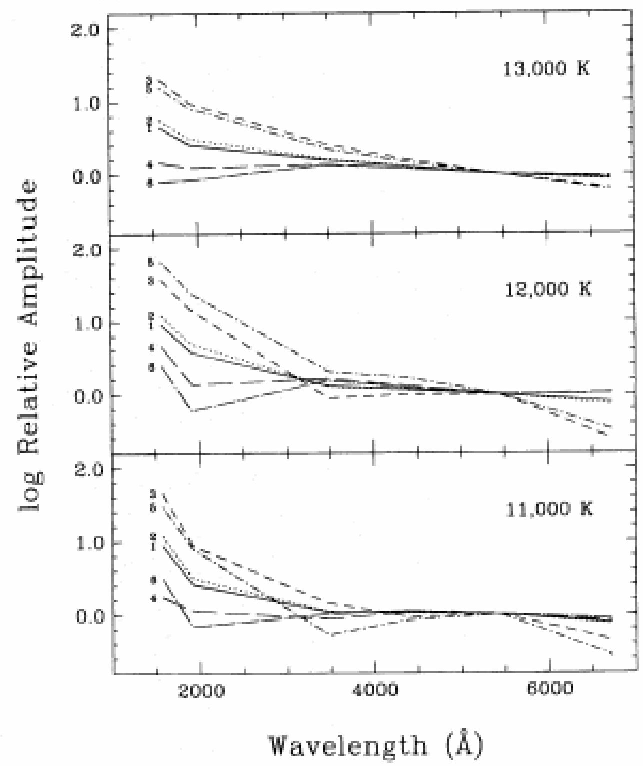

FIG. 2.—Normalized pulsation amplitudes for the six bandpasses of interest computed from ML1 model atmospheres with log $g = 8.0$ and with three different effective temperatures. The solid (dotted, dashed, long-dashed, dot-dashed, dot-long-dashed) curve corresponds to a g-mode with $l = 1$ (2, 3, 4, 5, 6).

Fontaine, G., et al. (1996)

Behavior of A_l^x for Different MLTs

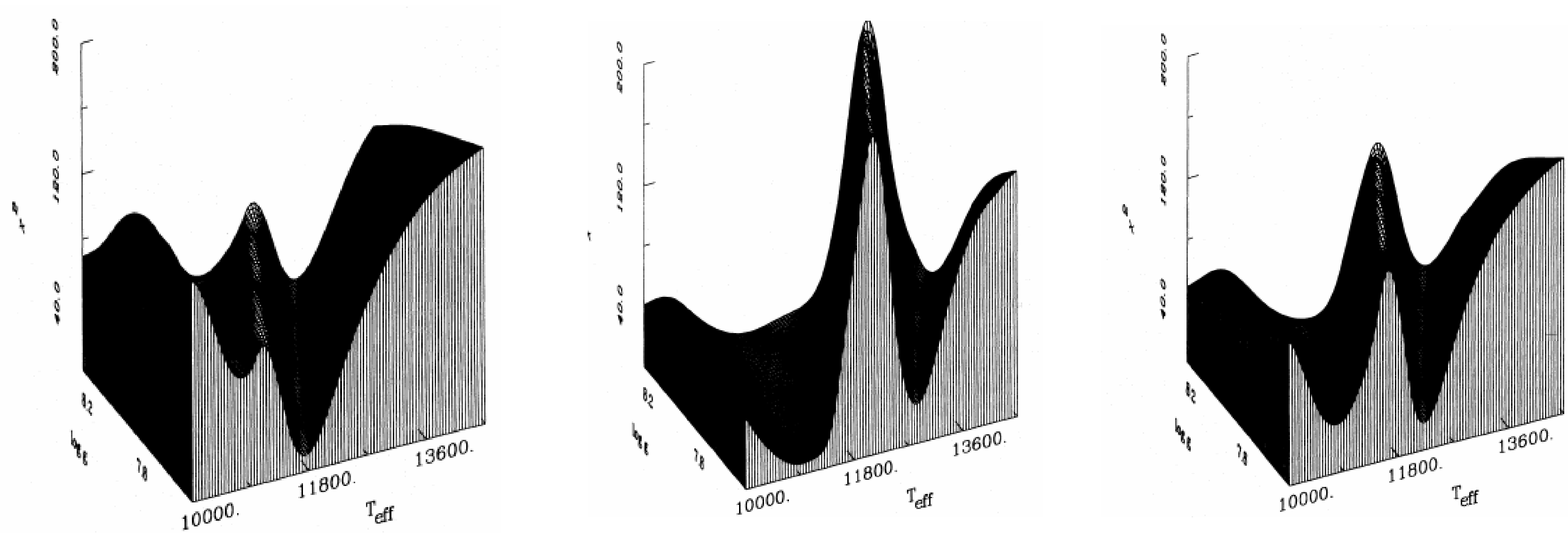

ML1 ML2 ML2/α=0.6

Fontaine, G., et al. (1996)

Behavior of A_l^x for Different MLTs

OPTIMAL SOLUTIONS FOR $l = 1$ AND $l = 2$

MLT (1)	log g (2)	T_{eff} ($l = 1$) (3)	χ^2 ($l = 1$) (4)	Filters[a] ($l = 1$) (5)	T_{eff} ($l = 2$) (6)	χ^2 ($l = 2$) (7)	Filters[a] ($l = 2$) (8)
ML2	7.50	10,950	6.937	...	10,950	12.21	*W*
	7.75	11,200	4.298	...	11,150	14.53	*W*
	8.00	11,450	3.890	...	11,350	14.68	*W*, *B*
	8.25	11,500	4.263	...	11,400	14.10	*B*
	8.50	11,750	4.533	...	11,700	13.62	*B*
ML2/$\alpha = 0.6$	7.50	12,200	18.05	*W*, *V*	12,400	33.20	*W**, *V**
	7.75	11,100	19.06	*U*, *V*	12,800	31.23	*W**, *V**
	8.00	11,350	14.61	*U*	13,250	31.37	*W**, *U*, *V**
	8.25	11,650	9.228	...	11,550	30.12	*M**, *W**, *B*
	8.50	12,050	7.256	...	12,000	29.19	*M*, *W**, *B*
ML1	7.50	11,750	9.919	*V*	11,950	33.64	*W**, *U*, *V**
	7.75	12,100	11.66	*V*	12,300	32.21	*W**, *U*, *V**
	8.00	12,500	14.83	*U*, *V*	12,700	33.17	*W*, *U**, *V**
	8.25	12,850	16.92	*W*, *U*, *V*	13,100	34.15	*W*, *U**, *V**
	8.50	13,300	20.35	*U*, *V*	13,550	35.14	*W*, *U**, *V**

[a] Letter alone indicates predicted pulsation amplitudes of more than 2 σ; letter with asterisk indicates predicted pulsation amplitudes of more than 3 σ.

Fontaine, G., et al. (1996)

The DAV Instability Strip

•Hotter group: Small number of short period modes.

•Cooler group: More modes, variable amplitudes, more non-linear effects (harmonics)

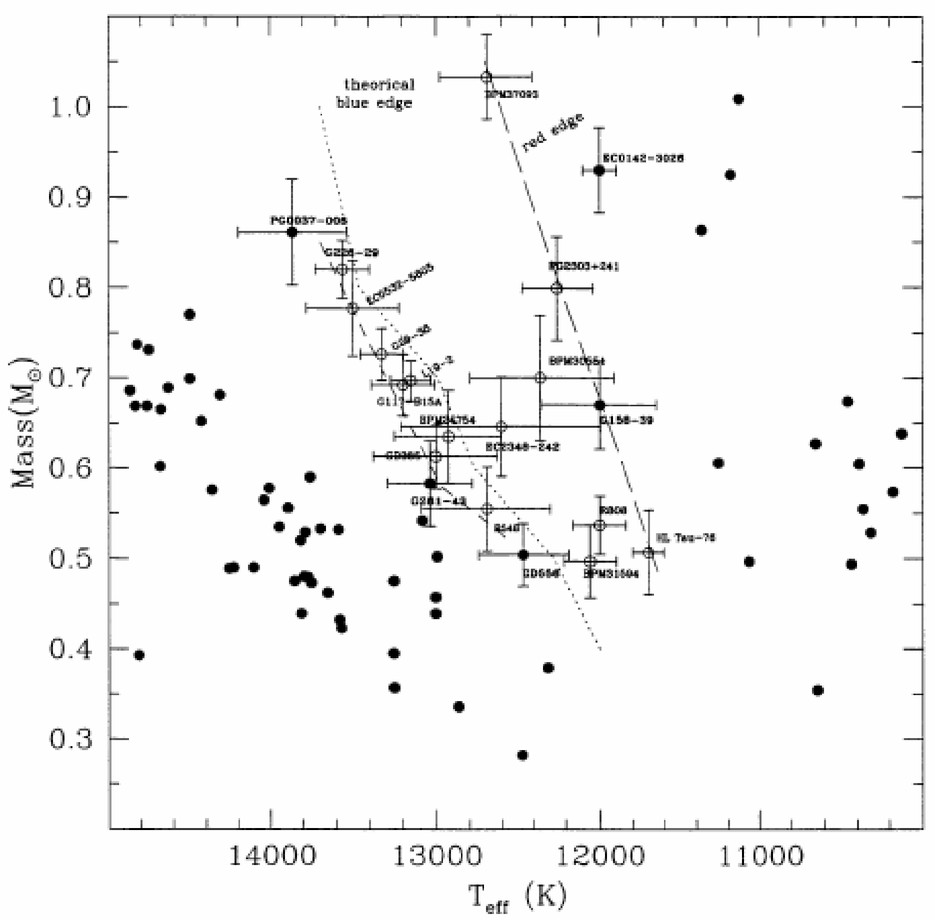

Kepler et al. (2000)

Spectra of DAVs

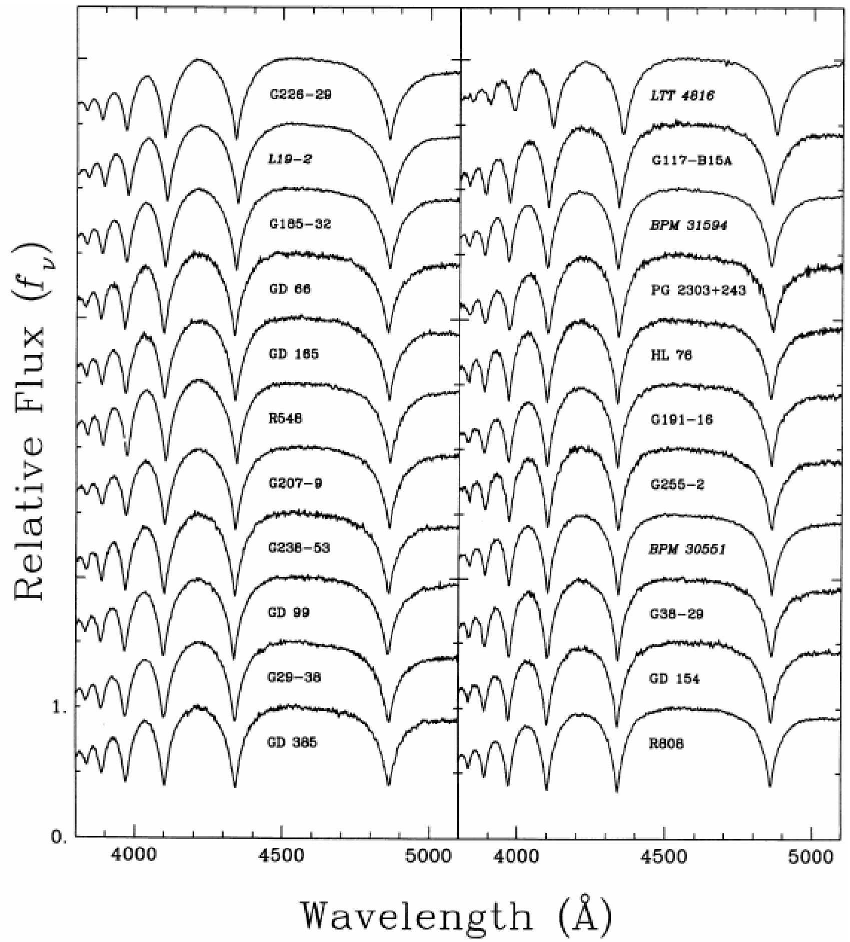

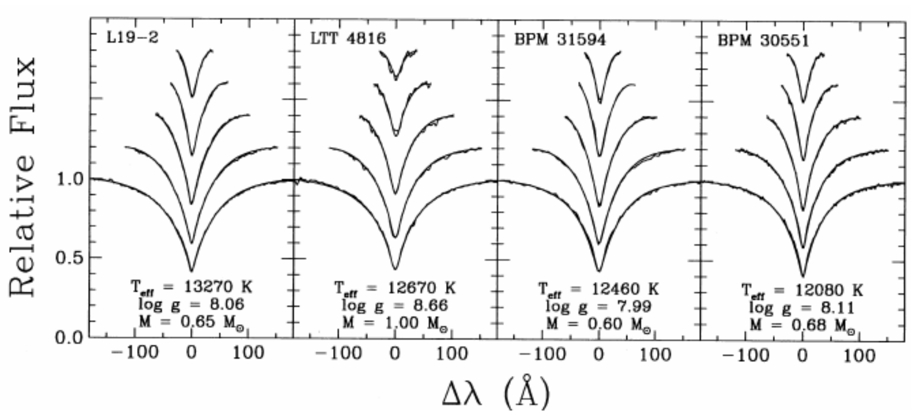

Bergeron, P., et al (1995)

Mass Dependence on MLTs

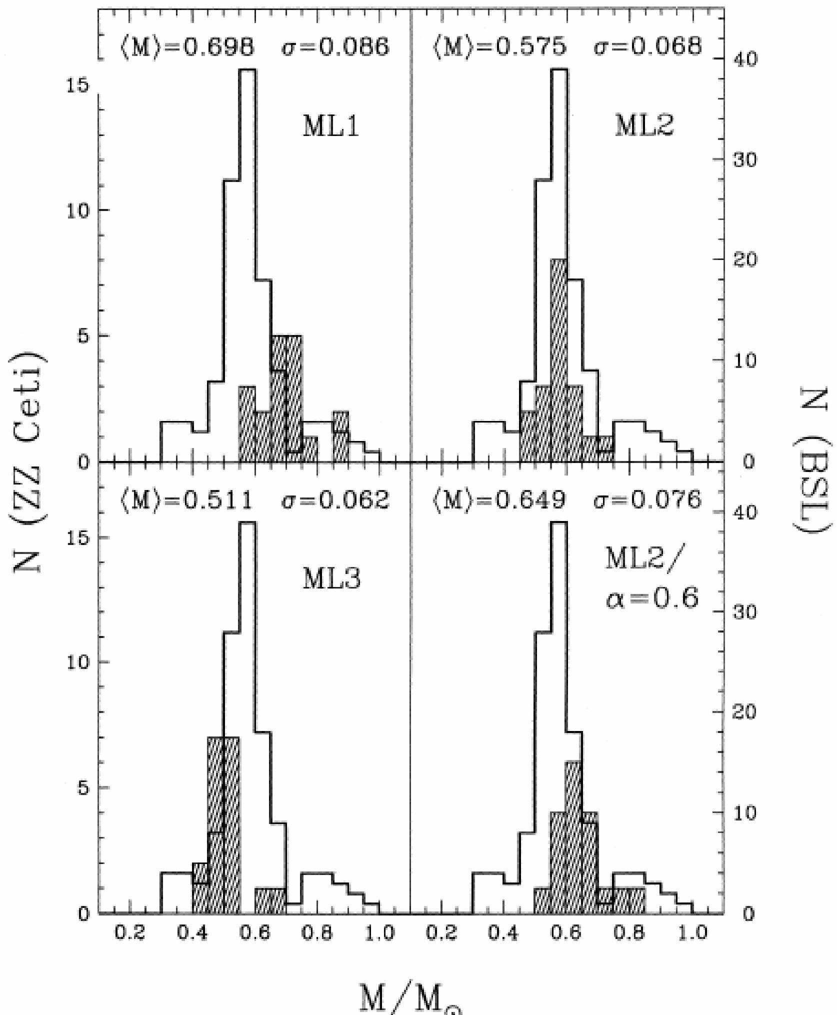

Bergeron, P., et al (1995)

Color-Color Diagrams and MLTs

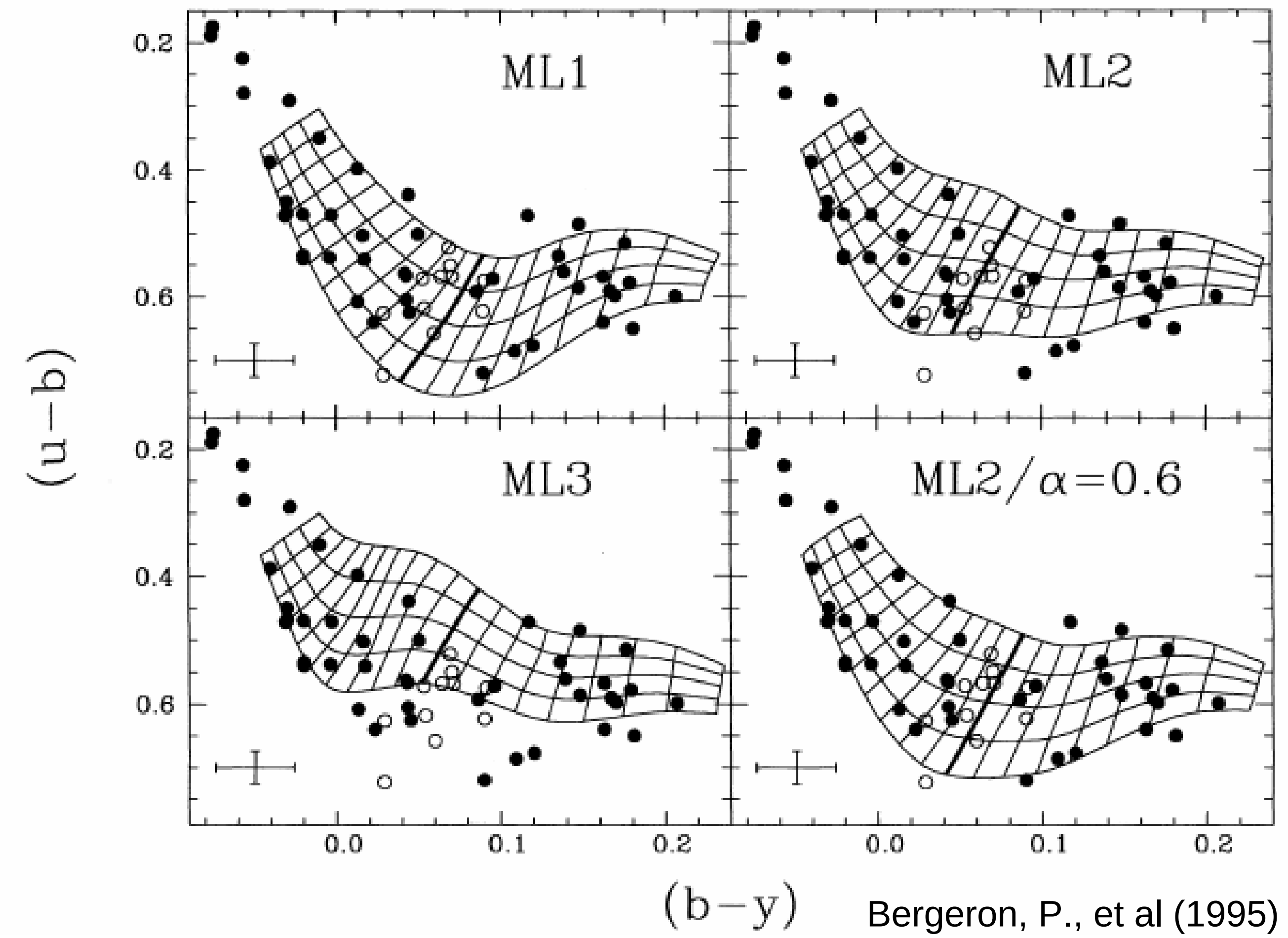

Bergeron, P., et al (1995)

T and g Dependence on MLTs

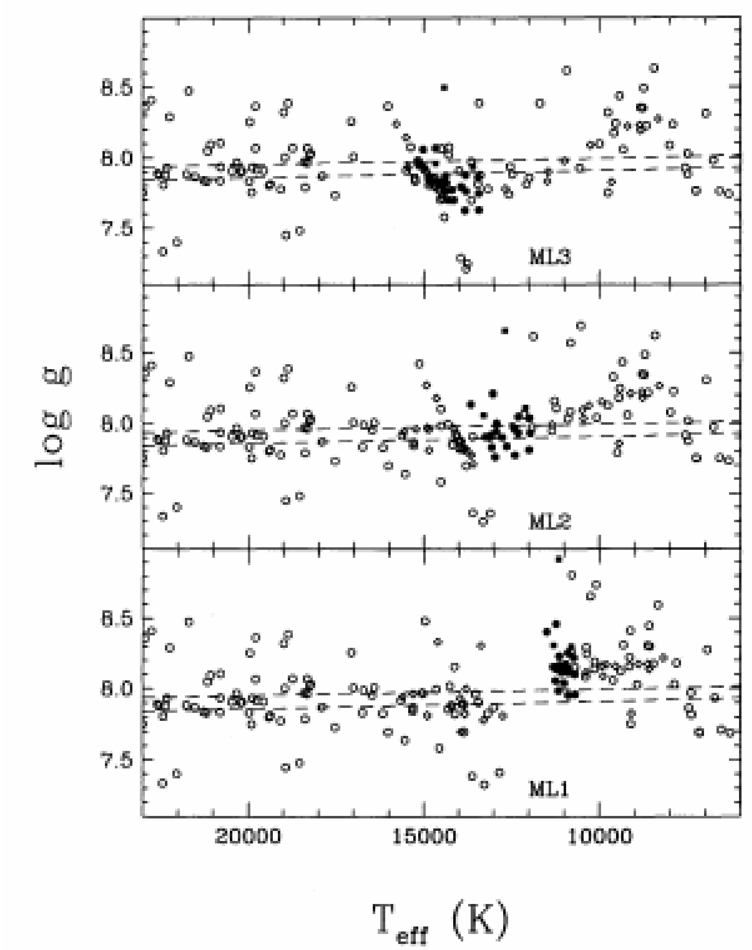

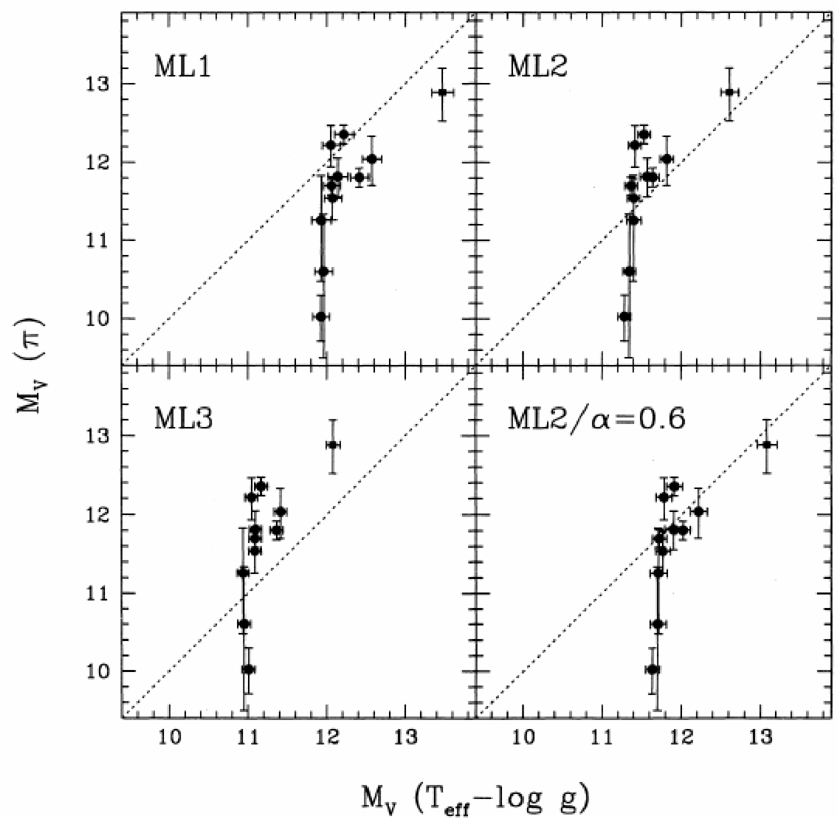

Bergeron, P., et al (1995)

T Dependence on MLTs

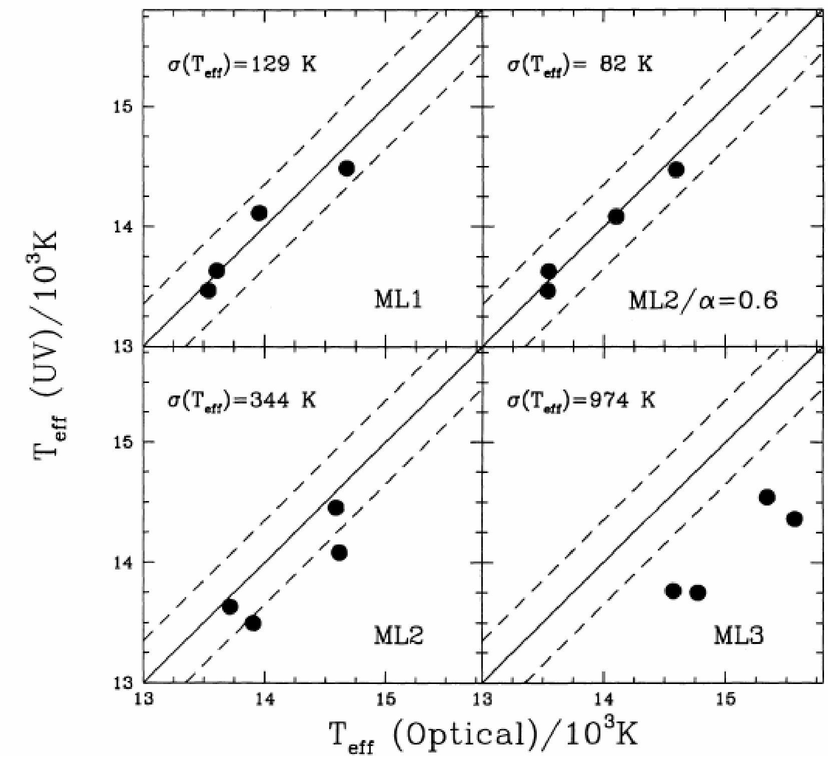

Atmospheric Parameters for the Kepler-Nelan DA Stars (ML2/α = 0.6)

WD	Name	T_{eff}/UV (K)	T_{eff}/Opt (K)	log g	$M/M_{\odot}$
0255−705......	BPM 2819	10961	10620	8.17	0.71
0401+250......	G8-8	12227	12120	8.02	0.62
1022+050......	LP 550-52	11779	11540	7.70	0.45
1053−550......	BPM 20383	12849:	13630	7.85	0.53

Bergeron, P., et al (1995)

T Dependence on MLTs

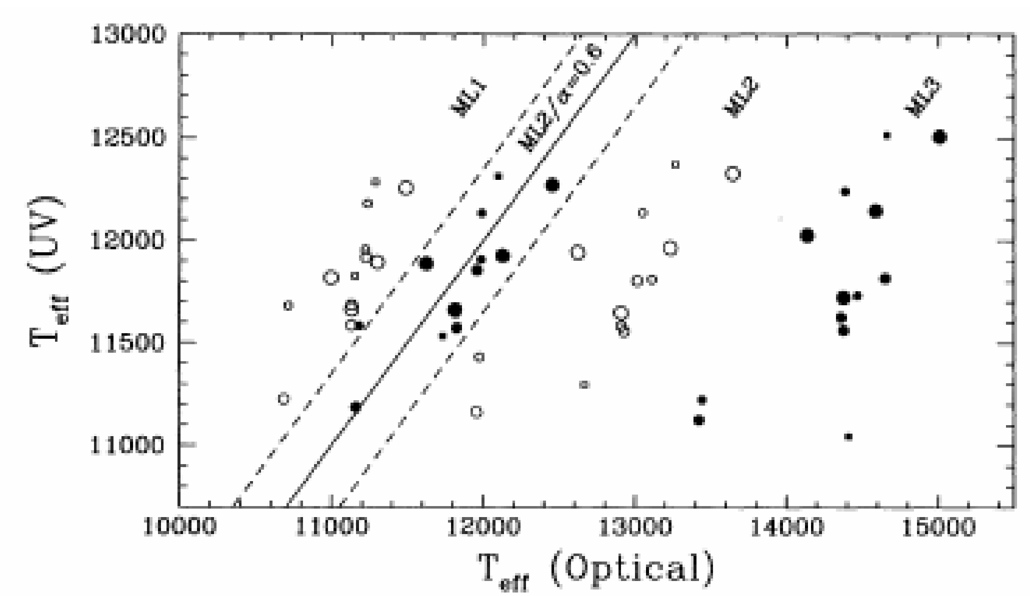

T_{eff} DETERMINATIONS FROM UV SPECTRA (ML2/α = 0.6)

Name	Source	T_{eff} (K)	ΔT_{eff} (UV − Opt)
G117-B15A	*HST*	11890	+270
G29-38	*IUE*	11660	−160
G226-29	*IUE*	12270	−190
G185-32	*IUE*	11930	−200
G29-38	*HST*	11650	−170
G207-9	*IUE*	11860	−100
GD 99	*IUE*	11570	−250
R808	*IUE*	11180	+20
R548	*IUE*	12130	+140
GD 154	*IUE*	11580	+400
GD 66	*IUE*	11910	−70
L19-2	*IUE*	12310	+210
LTT 4816	*IUE*	11530	−200

Bergeron, P., et al (1995)

Spectral Fits and the MLTs

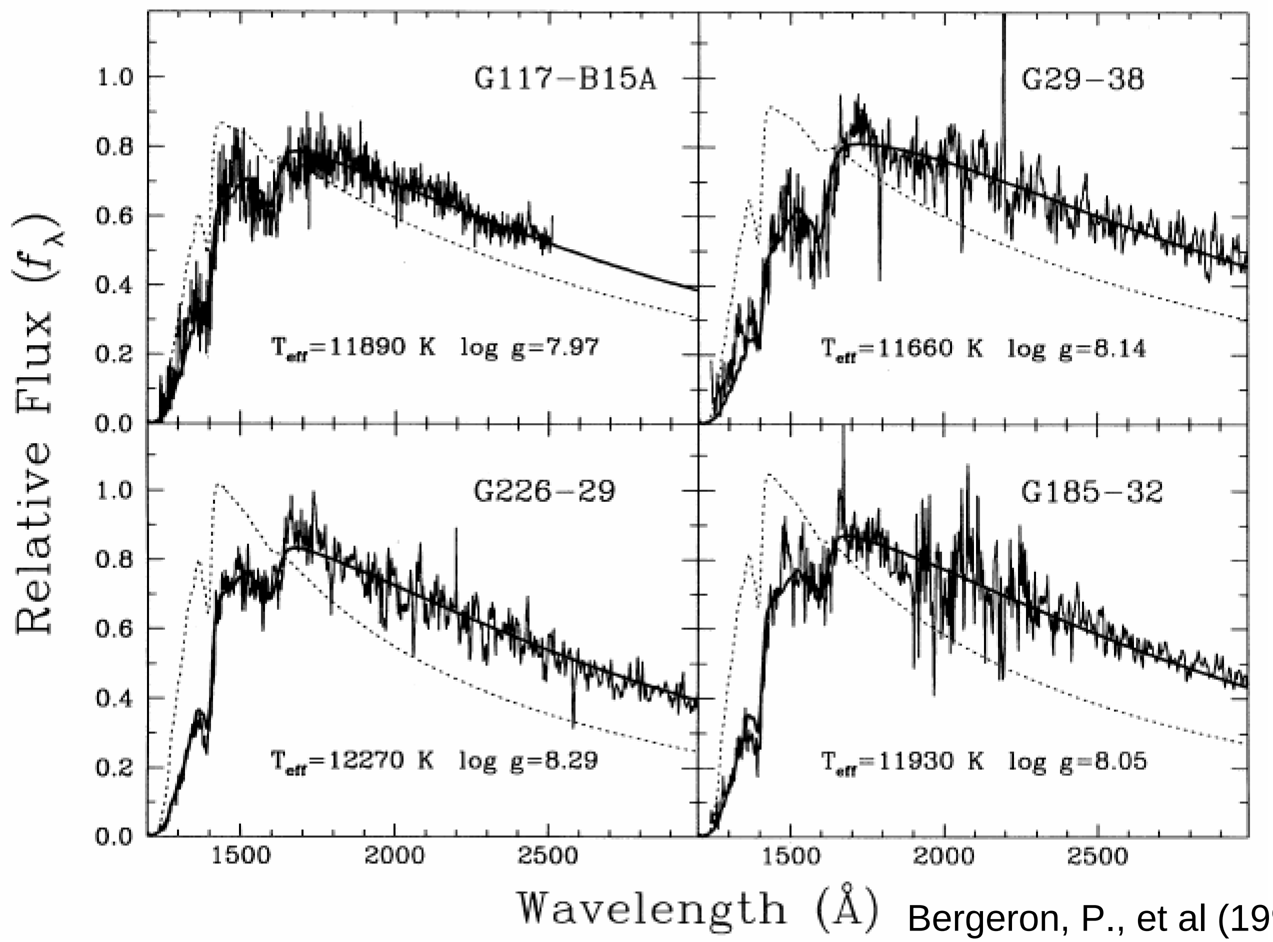

Bergeron, P., et al (1995)

Summary

- Three main categories of variable white dwarfs
- G-modes
- We can learn a lot from power spectra
- DAVs are harder to analyze with power spectra
- Can use spectroscopy
- All methods require a MLT assumption
- There are possible ways to reject/accept certain MLTs

Sources

- Bergeron, P., et al. 1995, ApJ, 449, 258
- Bradley, P.A. 1993, Baltic Astronomy, 2, 545
- Bradley, P.A. 1998, Baltic Astronomy, 7, 111
- Brassard, P., Fontaine, G., & Wesemael, F. 1995, ApJ 96, 545
- Costa, J.E.S., Kepler, S.O., & Winget, D.E. 1999, ApJ 522, 973
- Fontaine, G., et al. 1996, ApJ, 469, 320
- Hansen, C.J., Kawaler, S.D. & Trimble V. 2004. Stellar Interiors, 2nd ed., Springer-Verlag, NY.
- Kawaler, S.D., 1998, IAUS, 185, 261
- Kepler, S.O., et al. 2000, Baltic Astronomy, 9, 125
- Winget, D.E., et al. 1991, ApJ, 378, 326